

METABOLISM OF LIPID PEROXIDATION PRODUCT, 4-HYDROXYNONENAL (HNE) IN RAT ERYTHROCYTES: ROLE OF ALDOSE REDUCTASE

SANJAY SRIVASTAVA,* BHARAT L. DIXIT,[†] JIAN CAI,[‡] SILKY SHARMA,[†] HARRELL E. HURST,[‡]
ARUNI BHATNAGAR,*[‡] and SATISH K. SRIVASTAVA[†]

*Division of Cardiology, University of Louisville, Louisville, KY, USA; [†]Department of Human Biological Chemistry and Genetics, University of Texas Medical Branch, Galveston, TX, USA; and [‡]Department of Pharmacology and Toxicology, University of Louisville, Louisville, KY, USA

(Received 19 April 2000; Revised 6 June 2000; Accepted 8 June 2000)

Abstract—Lipid peroxidation represents a significant source of erythrocyte dysfunction and aging. Because the toxicity of lipid peroxidation appears to be in part due to aldehydic end products, we examined, in rat erythrocytes, the metabolism of 4-hydroxy-trans-2-nonenal (HNE), one of the most abundant and toxic lipid-derived aldehydes. Packed erythrocytes, 0.1 ml, completely metabolized 20 nmoles of HNE in 20 min. The glutathione conjugate of HNE and 4-hydroxynonanoic acid (HNA) represented 70 and 25% of the total metabolism, respectively. Approximately 70% of the metabolites were extruded to the medium. Upon electrospray ionization mass spectrometry, the glutathione conjugate resolved into two distinct species corresponding to glutathionyl HNE (GS-HNE) and glutathionyl 1,4-dihydroxynonene (GS-DHN). The concentration of GS-DHN formed was twice that of GS-HNE. Inhibition of aldose reductase by sorbinil and tolrestat led to a selective decrease in the formation of GS-DHN, although the extent of HNE glutathiolation was unaffected. Inhibitors of aldehyde or alcohol dehydrogenase, i.e., cyanamide and 4-methyl pyrazole, had no effect on the formation of HNA and GS-DHN, indicating that these enzymes are not significant participants in the erythrocyte HNE metabolism. Thus, oxidation to HNA, conjugation with glutathione, and further reduction of the conjugate by aldose reductase appear to be the major pathways of HNE metabolism in erythrocytes. These pathways may be critical determinants of erythrocyte toxicity due to lipid peroxidation-derived aldehydes. © 2000 Elsevier Science Inc.

Keywords—Lipid peroxidation, 4-hydroxy-trans-2-nonenal, Aldose reductase, Erythrocytes, Glutathione, Free radicals

INTRODUCTION

Lipid peroxidation has been suggested to play an important role in the etiology of several disease processes including atherosclerosis, ischemia/reperfusion, diabetes, cancer, and aging [1–3]. Oxidation of polyunsaturated fatty acids—containing phospholipids in tissues generates lipid hydroperoxides, which are further degraded to several products including saturated aldehydes such as hexanal and unsaturated aldehydes [e.g., malonaldehyde (MDA) and 4-hydroxy-trans-2-nonenal (HNE)]. Of these, the unsaturated aldehydes play an important role in

mediating the pathophysiological effects of oxidative stress [1–3]. Unlike their precursors, the reactive oxygen species, which generally have an extremely short half-life, the lipid-derived aldehydes are metastable and can diffuse from their site of origin and can, therefore, propagate oxidative injury by acting as “toxic second messengers”.

Of the various lipid peroxidation products, HNE, generated mainly from ω -6 polyunsaturated fatty acids such as arachidonic and linoleic acids, has received considerable attention due to its high bioactivity. The electrophilic nature of the α , β unsaturation in HNE renders it highly reactive with cellular nucleophiles such as glutathione, cysteine, lysine, and histidine of proteins, and with nucleic acids [3–5]. High concentrations of HNE are cytotoxic, whereas lower concentrations of HNE modulate cell proliferation and gene expression, inhibit

Address correspondence to: Dr. Satish K. Srivastava, Department of Human Biological Chemistry and Genetics, University of Texas Medical Branch, 6.644 Basic Science Building, Galveston, TX 77555-0647, USA; Tel: (409) 772-3926; Fax: (409) 772-9679; E-Mail: sssrivast@utmb.edu.

the synthesis of nucleic acids and proteins, stimulate neutrophil chemotaxis, and modulate platelet aggregation [3].

Erythrocytes are potential targets of lipid peroxidation products, generated endogenously within the cell or present in the environment. The high concentration of polyunsaturated fatty acids in the membrane phospholipids [6] provides a rich substratum for oxidants. The presence of transition metals capable of serving as redox agents, hemoglobin, and other heme-containing proteins, can also augment lipid peroxidation [7,8]. Extracellular oxidative damage occurs in the area of inflammation and atherosclerosis, where stimulated neutrophils [9,10] and endothelial cells [11,12] release reactive oxygen species capable of causing red cell membrane damage. High concentration of lipid peroxidation products including HNE have also been reported in erythrocytes of shock patients [13] and uremic subjects [14] and in the bone marrow of the rats subjected to total body irradiation [15]. The lipid peroxidation products such as HNE accumulate in the erythrocytes [16] and can cause covalent modification of the intrinsic proteins [17] and red cell lysis [18]. Metabolism of HNE to lesser reactive molecules is, therefore, a prerequisite to ensure the survival and normal functioning of erythrocytes. In the present study, we examined the contribution of the various metabolic pathways involved in the biotransformation of HNE in erythrocytes.

MATERIALS AND METHODS

Materials

Cyanamide, 4-methyl pyrazole (4-MP), aldehyde dehydrogenase, and glutathione (GSH) were purchased from Sigma Chemical Co. (St. Louis, MO, USA). Sorbinil and tolrestat were gifts from Pfizer (Groton, CT, USA) and Ayerst (Princeton, NJ, USA), respectively. All other reagents were of the highest purity available.

Chemical synthesis

[4-³H] HNE was synthesized as its dimethyl acetal as described earlier [19]. Prior to use, free [4-³H] HNE was obtained by the acid hydrolysis of the dimethyl acetal and purified by HPLC. The synthesized [4-³H] HNE had a specific activity of 75–100 mCi/mmol. Radiolabeled 1,4-dihydroxy-2-nonene (DHN) was synthesized enzymatically by incubating 0.1 μ mole of [4-³H] HNE with 0.5 units of human recombinant aldose reductase and 0.1 mM NADPH in 0.15 M potassium phosphate, pH 7.0, at 25°C. The reaction was monitored by following the decrease in absorbance at 224 nm.

At the end of the reaction, aldose reductase was

removed by ultrafiltration using an Amicon Centriprep-10 (Millipore, Bedford, MA, USA), and DHN in the filtrate was purified by HPLC as described below. The 4-hydroxy-2-nonenoic acid (HNA) was synthesized by incubating 0.1 μ mol of [4-³H] HNE with 1.5 units of yeast aldehyde dehydrogenase, 1.5 mM NAD, and 0.1 M potassium phosphate, pH 7.4, at 25°C. Oxidation of HNA was followed by the increase in absorbance at 340 nm due to NAD reduction. The protein in the reaction mixture was removed by ultrafiltration and HNA recovered in the filtrate was purified by HPLC. The identity and purity of the reagent HNE, DHN, and HNA were established by nuclear magnetic spectroscopy (NMR) and gas chromatography–chemical ionization mass spectroscopy (GC-CI/MS).

HPLC analysis

Synthesized standards and metabolites of HNE were separated by HPLC using a Varian reverse phase ODS C₁₈ column (Varian Analytical Instruments, Walnut Creek, CA, USA), pre-equilibrated with 0.1% trifluoroacetic acid (TFA) at a flow rate of 1 ml/min. The compounds were eluted using a gradient consisting of solvent A (0.1% aqueous trifluoroacetic acid, TFA) and solvent B (100% acetonitrile) at a flow rate of 1 ml/min. The gradient was established such that B reached 24% in 15 min and held at 24% for 5 min. In an additional 10 min, B reached 26% and was held at this value for 5 min. Further, in the next 10 min solvent B reached 60%, and in an additional 10 min, it reached 100%. In this system, the glutathione conjugates (GS-HNE and GS-DHN) elute with a retention time (τ_R) of approximately 17 min, whereas DHN, HNA, and HNE have a τ_R of 26, 32, and 37 min, respectively (Fig. 1).

Mass spectrometry

ESI⁺/MS analyses were performed on a single quadrupole Micromass LCZ instrument. The ESI⁺/MS operating parameters were as follows: capillary voltage, 3.0 kV; cone voltage, 25 V; extractor voltage, 4 V; source block temperature, 80°C; and dissolution temperature, 200°C. Nitrogen at 3 psi was used as nebulizer gas. Samples were reconstituted in 100 μ l acetonitrile/water/acetic acid 50/50/0.1 (v/v/v), and then introduced into the mass spectrophotometer using a Harvard syringe pump at a rate of 10 μ l/min. Spectra were acquired at the rate of 200 atomic mass units/s over the range of 100–650 atomic mass units.

Gas chromatography–chemical ionization mass spectrometry (GC-CI/MS)

For GC-CI/MS analyses, the samples were derivatized in 20 μ l of acetonitrile with 20 μ l of N,O-

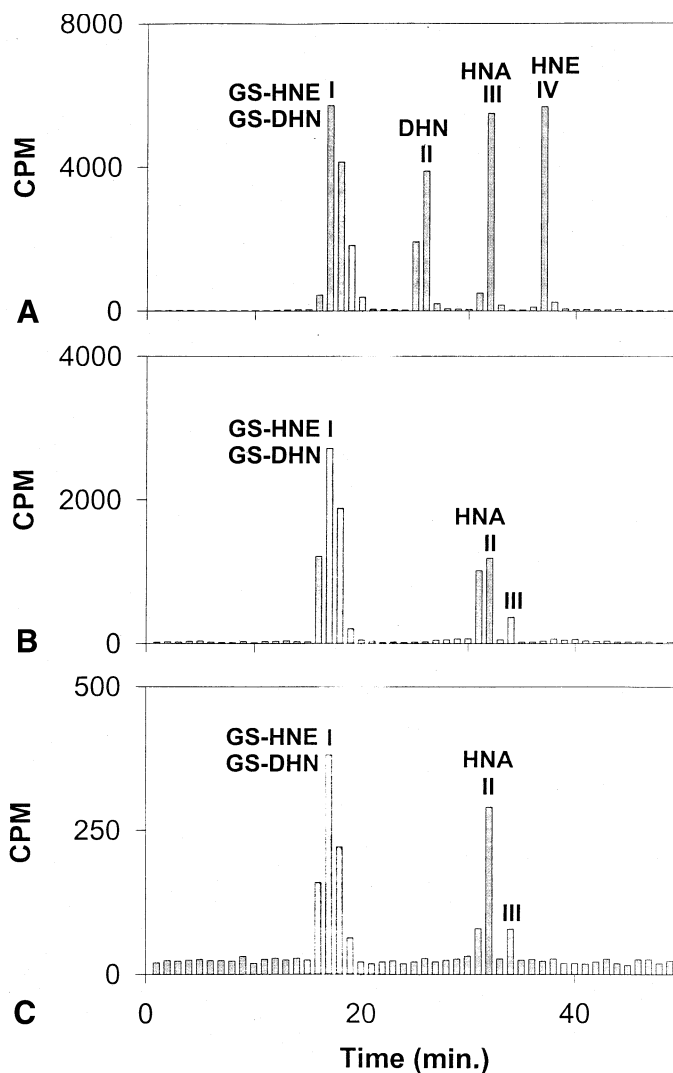


Fig. 1. (A) HPLC profile of synthesized putative metabolites of $[4\text{-}^3\text{H}]$ HNE. Tritiated HNE, DHN, HNA, GS-HNE, and GS-DHN were synthesized as described under Materials and Methods. Each metabolite containing approximately 7000 cpm (≈ 4 nmoles) was reconstituted in KH buffer and applied to ODS C_{18} reverse phase HPLC column. One milliliter fractions of the eluate were collected every minute and radioactivity was measured in each fraction. Retention time (τ_R) was found to be 17 min for the glutathione conjugates GS-HNE and GS-DHN (peak I), 26 min for DHN (peak II), 32 min for HNA (peak III), and 37 min for HNE (peak IV). (B) HPLC profile of radiolabeled metabolites of $[4\text{-}^3\text{H}]$ HNE in the incubation media of rat erythrocytes treated with HNE. The erythrocytes were incubated with 20 nmoles of $[4\text{-}^3\text{H}]$ HNE in 1.0 ml KH buffer. After 30 min at 37°C , the incubation media was collected, centrifuged at $10,000 \times g$ for 10 min, and ultrafiltered. The radioactivity collected in the medium was measured and separated by HPLC using an ODS C_{18} column. One milliliter fractions were collected and $100 \mu\text{l}$ were used to measure the radioactivity. The peaks I–III are marked. Peak I corresponds to the reagent glutathione conjugates of HNE, peak II corresponds to HNA, and the identity of peak III is not known. (C) Erythrocytes incubated with $[4\text{-}^3\text{H}]$ HNE as above were separated from the incubation media after 30 min and the cells were lysed with deionized water. Hemolysates were ultrafiltered and purified on HPLC. The peaks at 17 min and 32 min correspond to glutathionyl conjugates of HNE and HNA, respectively.

bis(trimethylsilyl)-trifluoroacetamide (BSTFA) for 1 h at 60°C . The mixture was cooled to room temperature and $2 \mu\text{l}$ aliquots were used for analysis. The GC-MS analysis was performed using a HP5890/HP5973 GC/MS system (Hewlett Packard; Palo Alto, CA, USA) under 70 eV electron ionization conditions. The compounds were separated on a bonded phase capillary column (DB-5MS, $30 \text{ m} \times 0.25 \text{ mm ID} \times$

$0.25 \mu\text{m}$ film thickness from J7W Scientific Folsom, CA, USA. The GC injection port and interface temperature were set to 280°C , with helium gas (carrier) maintained at 14 psi. Injections were made in the splitless mode with the inlet port purged for 1 min following injection. The GC oven temperature was held initially at 100°C for 1 min, then increased at a rate of $10^\circ\text{C min}^{-1}$ to 280°C , which was held for 5 min.

Under these conditions, the retention time for HNA derivative was 9.67 min.

Metabolic studies

Rat blood, withdrawn by heart puncture using 3.8% trisodium citrate as anticoagulant (1 ml sodium citrate: 9 ml blood) was centrifuged at $1000 \times g$ for 15 min at 4°C and plasma and the buffy coat were removed by aspiration. The erythrocytes were washed three times with 5–7 volumes of phosphate-buffered saline (PBS; 0.1 M phosphate containing 0.9% sodium chloride, pH 7.4) and finally with the Krebs-Hansleit (KH) buffer containing (in mM) NaCl, 118; KCl, 4.7; MgCl_2 , 1.25; CaCl_2 , 3.0; KH_2PO_4 , 1.25; EDTA, 0.5; NaHCO_3 , 25; and glucose, 10, pH 7.4. Washed erythrocytes were resuspended in KH buffer and were used within 1 h. Initial experiments described the time course of HNE metabolism. Washed erythrocytes (100 μl ; approximately 2×10^8 cells) were incubated with 20 nmoles of $[4\text{-}^3\text{H}]$ HNE in 1.0 ml KH buffer. Aliquots were withdrawn at indicated times, centrifuged at $10,000 \times g$ for 10 min at 4°C , and the supernatant was ultrafiltered by centrifugation using Amicon centiprep-10 and applied to a Varian ODS C_{18} reverse phase column. The pellet was washed three times with KH buffer and hemolysed by adding deionized water. The hemolysate was ultrafiltered and applied to Varian ODS C_{18} reverse phase column. The metabolites of $[4\text{-}^3\text{H}]$ HNE were quantitated by determining radioactivity in each fraction and individual peaks were analyzed by ESI^+/MS or $\text{GC-Cl}/\text{MS}$.

Inhibition of oxidoreductases

Washed erythrocytes, 100 μl packed cells, were incubated in 1.0 ml KH buffer without or with 0.2 or 1.0 mM sorbinil, 0.01 mM tolrestat, 0.5 mM 4-MP, or 2.0 mM cyanamide for 30 min at 37°C . $[4\text{-}^3\text{H}]$ HNE, 20 nmoles, were then added in the incubation media of each sample and the incubation was carried out for an additional 30 min at 37°C . After the incubation, erythrocytes were separated from the media and the samples were processed as described above.

RESULTS

HNE consumption

When 0.1 ml erythrocytes were incubated with 20 μM $[4\text{-}^3\text{H}]$ HNE in 1.0 ml KH buffer, approximately 80% HNE was metabolized within 5 min and no unmetabolized HNE was detected in the incubation media after 20 min (Table 1). After 30 min of incubation of the erythrocytes with $[^3\text{H}]$ -HNE, $70 \pm 8\%$ of the total radioac-

Table 1. Percent Distribution of Metabolites Recovered in the Incubation Medium from Rat Erythrocytes Incubated with $[4\text{-}^3\text{H}]$ HNE

Incubation time (min)	Peak I (glutathione-conjugates)	Peak II (HNA)	Peak III	Peak IV (HNE)
2	48	10	2	40
5	61	18	4	17
10	68	21	4	7
20	68	28	4	—
30	70	25	5	—

Rat erythrocytes (0.1 ml) were incubated with 20 nmoles $[4\text{-}^3\text{H}]$ HNE and the metabolites present in the incubation media were separated by HPLC as described in the text. The results are given as percentage of the total radioactivity recovered from HPLC.

tivity was recovered in the incubation medium, $10 \pm 4\%$ radioactivity was recovered in the hemolysate, and $< 1\%$ radioactivity was found to be protein-bound. Radioactive peaks obtained by the HPLC separation of the incubation media, were assigned to various HNE metabolites and unmetabolized HNE on the basis of the τ_{R} of the synthesized standards (Fig. 1).

The τ_{R} of Peak I of the incubation medium, representing approximately 70% radioactivity, recovered in the medium, was identical to reagent glutathionyl conjugates of HNE (GS-HNE) and its reduced form (GS-DHN). The τ_{R} of Peak II, representing 25% radioactivity, corresponded to reagent HNA. Another minor peak (5% of the radioactivity), observed at τ_{R} of 34 min was not identified. To identify the glutathione conjugates, putative conjugates were synthesized and purified by HPLC. GS-HNE was synthesized by incubating 0.1 μmole of HNE with 5-fold excess of GSH in 0.1 M K-phosphate, pH 7.4, at 25°C . GS-HNE thus formed was purified on HPLC, dried on Speed Vac, and reconstituted in acetonitrile:water:acetic acid 50/50/0.1% (v/v/v). In this solution, ESI/MS of the GS-HNE conjugate showed a pseudo-molecular ion $[\text{M} + \text{H}]^+$ with a m/z of 464. An additional species with m/z 446 was also observed (Fig. 2A). The relative abundance of this ion varied with the cone voltage and temperature. At low cone voltages and low temperatures, the 446 species disappeared with concomitant increase in the 464 species (Fig. 2B), indicating that the 446 species is a daughter ion arising from the loss of a single water molecule from the parent 464 ion.

The reduced form of the GS-HNE conjugate (GS-DHN), synthesized by aldose reductase-catalyzed reduction of GS-HNE using NADPH as a cosubstrate, was purified on HPLC and reconstituted in electrospray solvent as described above. Upon ESI^+/MS , GS-DHN displayed a single pseudo-molecular ion $[\text{M} + \text{H}]^+$ with a m/z of 466. No daughter ion due to dehydration of the parent ion was observed (Fig. 2C). Peaks with m/z of 464 and 446 are due to nonreduced GS-HNE.

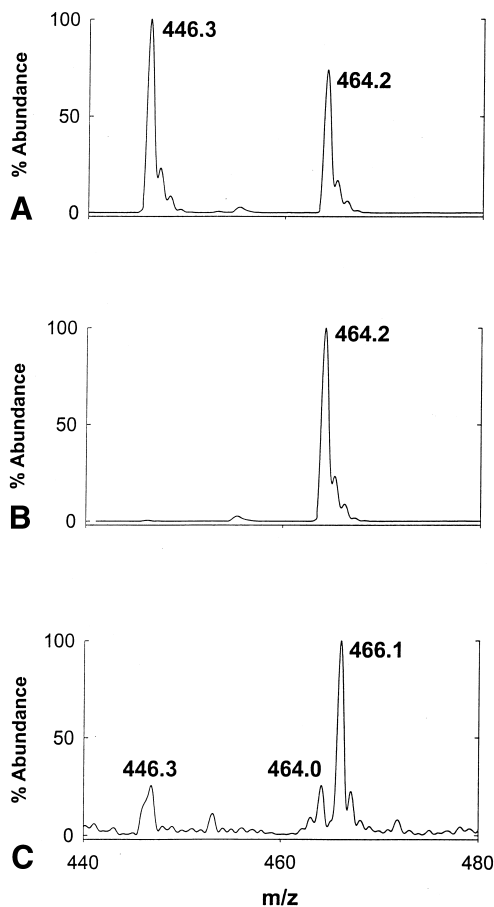


Fig. 2. ESI⁺-mass spectrum of reagent GS-HNE and GS-DHN. Glutathione conjugates of HNE and DHN were synthesized and purified on HPLC and injected into electrospray as described under Materials and Methods. (A) Spectrum of GS-HNE: ESI⁺-mass spectra was acquired at the cone voltage of 25 V and source block and dissolution temperatures were 80 and 200°C, respectively. The peak at *m/z* 464.2 was assigned to the parent ion, whereas peak at 446.3 was assigned to the daughter ion originating from in-source dehydration of the parent ion. (B) ESI⁺-mass spectra of GS-HNE was acquired at 17 V and the source block and dissolution temperatures were 50 and 100°C, respectively. Under these conditions, the *m/z* value of GS-HNE was 464.2. (C) ESI⁺-mass spectrum of GS-DHN: the tune parameters were identical to (A). Under these conditions, the parent ion of GS-DHN forms a well-resolved ion with *m/z* 466.1. The ions with *m/z* 464.0 and 446.3 appear to be due to the residual GS-HNE in the reaction mixture and its dehydrated form, respectively.

ESI⁺/MS of Peak I, obtained from HNE metabolites of erythrocytes in the incubation medium, showed a predominant ion with *m/z* 466.1, which was assigned to +1 charge state of GS-DHN (Fig. 3A). The ion with *m/z* 464.1 corresponded to the +1 charge state of GS-HNE. This ion represented 25% of the GS-DHN signal. An additional species with *m/z* 446.4 was ascribed to dehydrated GS-HNE [M-18], since a similar ion was observed with reagent GS-HNE. The ion with *m/z* 446 accounted for approximately 25% of GS-DHN signal. The distribution of the molecular ions shows that relative abun-

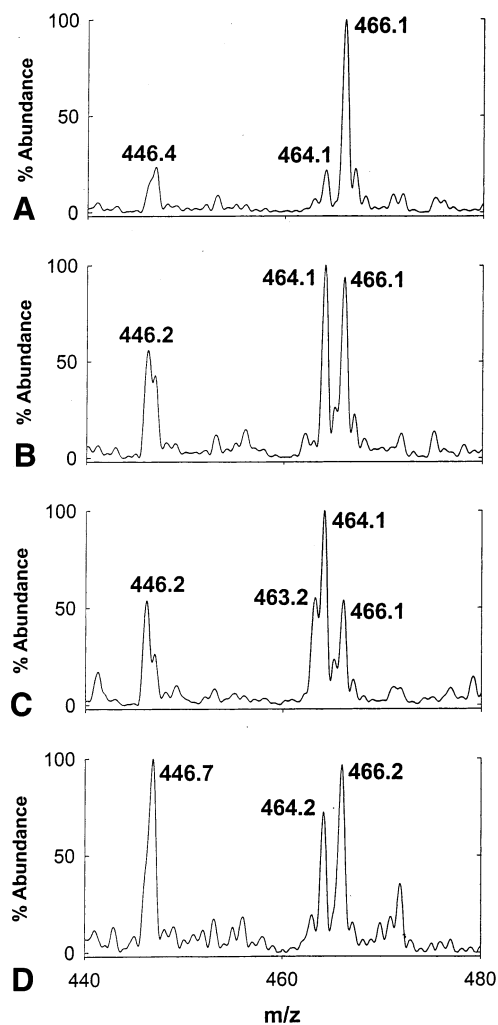


Fig. 3. Rat erythrocytes (0.1 ml) were incubated (A) without inhibitors, or with (B) sorbiniol (0.2 mM), (C) sorbiniol (1.0 mM), or (D) tolrestat (0.01 mM) in 1.0 ml KH buffer for 30 min at 37°C, after which 20 nmoles [4-³H] HNE were added to the incubation media, and the flasks were incubated for an additional 30 min. Metabolites in the incubation media were separated on HPLC and fractions corresponding to Peak I were analyzed by ESI⁺/MS. ESI⁺/MS conditions were same as in Fig. 2A.

dance of GS-DHN 67% and that of GS-HNE was 33%, indicating that the extruded conjugate is predominantly in the reduced form.

Peak II of the incubation medium was characterized by GC-CI/MS. Fractions corresponding to this peak were pooled, silylated, and subjected to GC-CI/MS. The gas chromatograph showed a prominent solvent-independent peak with a τ_R identical to reagent HNA (Fig. 4). Fragmentation pattern of this ion was found to be identical to that of synthetic HNA, indicating the presence of HNA in Peak II.

The HPLC separation of hemolysate of the HNE-treated erythrocytes also yielded three radioactive peaks at τ_R =17, 32, and 34 min (Table 2). Peak I correspond-

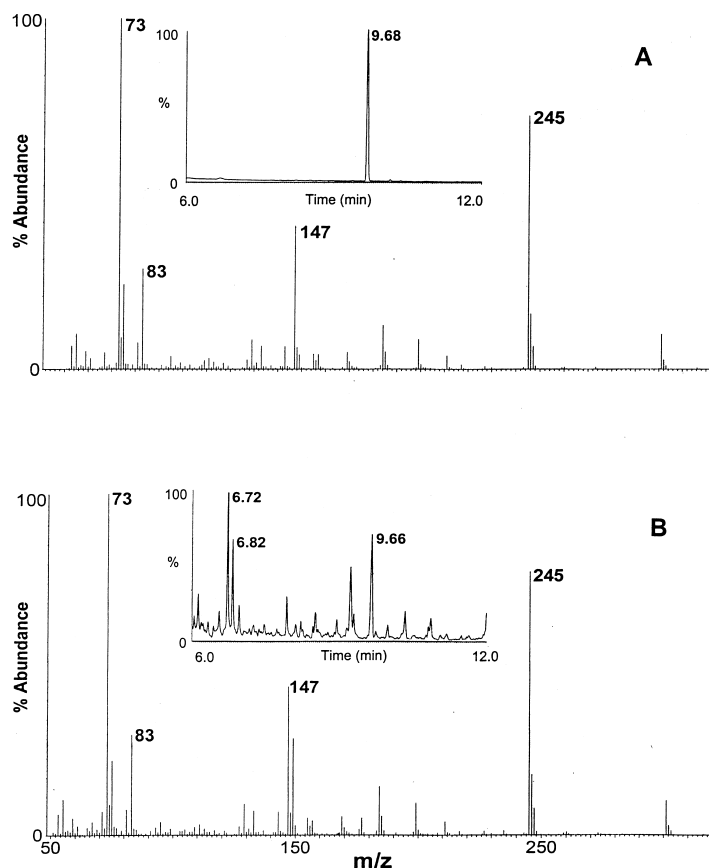


Fig. 4. GC/CI-mass spectrum of reagent HNA. (A) Reagent HNA derivatized with BSTFA eluted at $t = 9.68$ min on GC (inset). The positive ionization mass spectrum shows the indicated derivatives at m/z 73, 83, 147, and 245. (B) GC-spectrum of Peak II obtained from HPLC separation of tritiated metabolites in the incubation media, extruded by the rat erythrocytes treated with $[4\text{-}^3\text{H}]$ HNE. Fractions corresponding to peak II were pooled, derivatized, and subjected to GC/CI-mass spectroscopy. Peak with the retention time of 9.66 min corresponds to reagent HNA (inset). The positive ionization mass spectrum of this peak shows the indicated derivatives of HNA at m/z 73, 83, 147, and 245.

ing to the glutathione conjugates, accounted for $65 \pm 11\%$ of the total radioactivity in the hemolysate. ESI⁺/MS of this peak showed that the relative abundance of GS-DHN and GS-HNE was similar to that in

the incubation media. Peak II of the hemolysate accounted for $30 \pm 5\%$ of the total radioactivity recovered in the hemolysate. The τ_R of this peak was identical to reagent HNA and was, therefore, ascribed to HNA. Peak

Table 2. Effect of Oxidoreductase Inhibitors on HNE Metabolism in Rat Erythrocytes

Additives	Incubation media			Hemolysate		
	Peak I (glutathione-conjugates)	Peak II (HNA)	Peak III (Unknown)	Peak I (glutathione-conjugates)	Peak II (HNA)	Peak III (Unknown)
None	69 ± 7	26 ± 5	5 ± 3	65 ± 11	30 ± 5	5 ± 3
Sorbinil (0.2 mM)	66 ± 8	27 ± 6	7 ± 2	60 ± 15	27 ± 12	13 ± 8
Sorbinil (1.0 mM)	68 ± 9	26 ± 6	6 ± 2	68 ± 9	26 ± 6	6 ± 2
Tolrestat (10 μM)	64 ± 9	28 ± 5	8 ± 4	64 ± 11	23 ± 6	13 ± 9
4-MP (0.5 mM)	64 ± 7	31 ± 5	5 ± 2	66 ± 12	27 ± 7	7 ± 3
Cyanamide (2.0 mM)	68 ± 7	29 ± 6	3 ± 3	71 ± 13	24 ± 8	5 ± 3

Rat erythrocytes were incubated with the indicated additives for 30 min at 37°C. After equilibrium, 20 nmols of $[4\text{-}^3\text{H}]$ HNE were then added to the samples and the incubation was continued for an additional 30 min. The cells were separated from the incubation media and lysed with deionized water. Hemolysate and incubation media were separated on HPLC as described in the text. The results are the average \pm standard deviation of percentage of the total radioactivity recovered from HPLC of 3 samples.

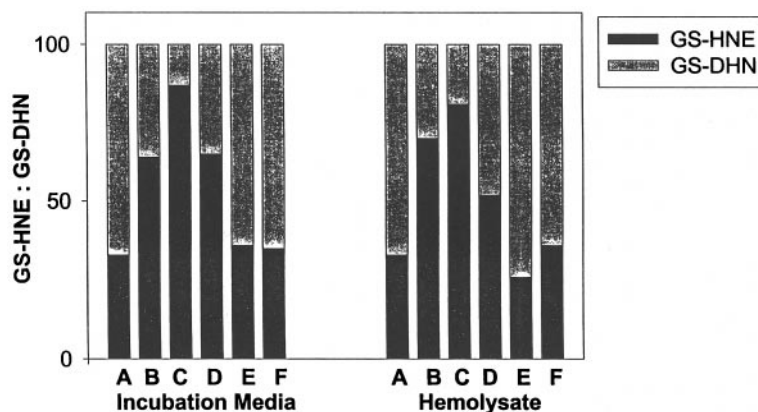


Fig. 5. Effect of oxidoreductase inhibition on GS-DHN formation. Rat erythrocytes (0.1 ml) were incubated (A) without inhibitors, or with (B) sorbinil (0.2 mM), (C) sorbinil (1.0 mM), (D) tolrestat (0.01 mM), (E) 0.5 mM 4-methyl pyrazole, or (F) 2.0 mM cyanamide in 1.0 ml KH buffer for 30 min at 37°C, after which 20 nmoles [$4\text{-}^3\text{H}$] HNE were added to the incubation media, and the flasks were incubated for an additional 30 min. Metabolites in the incubation media and hemolysate were separated on HPLC and fractions corresponding to Peak I were analyzed by ESI⁺/MS. ESI⁺/MS conditions were same as in Fig. 2A.

III of the hemolysate with a $\tau_R = 34$ min contained $5 \pm 3\%$ of the total radioactivity of the hemolysate and was not further characterized.

Identification of the metabolic pathways

The HPLC and mass spectroscopic analyses described above clearly demonstrate that the major metabolic products of HNE in erythrocytes are: GS-HNE, GS-DHN, and HNA. To identify the biochemical pathways involved in the formation of these metabolites, the erythrocytes were incubated for 30 min at 37°C without or with the inhibitors of aldose reductase, alcohol dehydrogenase, or aldehyde dehydrogenase in 1.0 ml KH buffer. After 30 min, 20 nmoles of [$4\text{-}^3\text{H}$] HNE were added to the medium, and the incubation was continued for an additional 30 min.

In the presence of the aldose reductase inhibitor, sorbinil (0.2 mM), radioactivity in the incubation medium upon HPLC separated into 3 peaks (Table 2). Peak I, with a τ_R corresponding to glutathione conjugates, accounted for $66 \pm 8\%$; peak II, corresponding to τ_R of HNA, accounted for $27 \pm 6\%$; and peak III ($\tau_R = 34$ min) accounted for $7 \pm 2\%$ of the total radioactivity recovered in the incubation medium.

The ESI-mass spectrum of peak I, obtained from sorbinil-treated cells, display a prominent ion with m/z 466.1, corresponding to $[\text{M}+\text{H}]^+$ of GS-DHN (Fig. 3B). Additional ions, observed at m/z 464.1 and 446.2 were assigned to $[\text{M}+\text{H}]^+$ of GS-HNE and its dehydrated $[\text{M}-18]$ daughter ion, respectively. Although the concentration of total conjugate (GS-DHN + GS-HNE) did not alter, the relative abundance of GS-DHN decreased from 67 to 36% and the GS-HNE increased from 33 to 64%

(Fig. 5). Together the peaks due to GS-HNE accounted for a signal, roughly 1.5-fold of that due to GS-DHN. Increasing the concentration of sorbinil in the incubation medium to 1.0 mM increased the abundance of ions with m/z 464 and 446 species with a simultaneous decrease in the 466 species, suggesting a significant inhibition of the reduction of the glutathionyl conjugate of HNE by sorbinil (Figs. 3C and 5).

From these data, we infer that in the presence of 1 mM sorbinil, the extruded conjugate is predominantly (87%) in the nonreduced form (GS-HNE). To confirm these observations further, we examined the effects of tolrestat (10 58 M), which represents a separate structural class of aldose reductase inhibitors [28]. The elution pattern of the HNE metabolites in the presence of tolrestat was similar to that obtained with sorbinil-treated cells (Table 2). Moreover, the ESI-mass spectrum of peak I of the metabolites obtained from tolrestat-treated cells showed strong signals corresponding to GS-DHN and GS-HNE (Fig. 3D). The relative abundance of GS-DHN (466 species) and GS-HNE (464 and 446 species) was 35 and 65%, respectively. Thus, treatment of cells with two structurally unrelated inhibitors of aldose reductase, sorbinil, and tolrestat resulted in the appearance of a relatively higher proportion of GS-HNE in the incubation medium, indicating that reduction of GS-HNE to GS-DHN is catalyzed by aldose reductase. Similar to the incubation medium, the reduction of GS-HNE to GS-DHN in the hemolysate of the erythrocytes was also significantly inhibited by aldose reductase inhibitors (sorbinil and tolrestat) (Fig. 5).

Incubation of the erythrocytes with 0.5 mM alcohol dehydrogenase inhibitor, 4-MP, had no significant effect on the rate of HNE metabolism or the HPLC elution

pattern of the HNE metabolites (Table 2). Furthermore, no inhibition of GS-DHN formation was observed in 4-MP-treated cells, both in the incubation media as well as hemolysate (Fig. 5), indicating that the reduction of GS-HNE to GS-DHN in erythrocytes is not catalyzed by alcohol dehydrogenase.

In most of the cells, oxidation of HNE to HNA is believed to be catalyzed by aldehyde dehydrogenase. Therefore, we investigated the effect of aldehyde dehydrogenase inhibitor, cyanamide, on the metabolism of HNE in rat erythrocytes. However, as shown in Table 2, cyanamide did not prevent HNE oxidation suggesting that in erythrocytes aldehyde dehydrogenase is not involved in the oxidation of HNE to HNA.

DISCUSSION

Erythrocytes are constantly exposed to reactive oxygen species both from intracellular as well as extrinsic sources. Observations of increased formation of lipid peroxidation-derived aldehydes during pathological oxidative stress necessitates their efficient metabolism to ensure the normal functioning of the cells. The normal physiological concentrations of HNE in the plasma and erythrocytes of humans and experimental animals have been reported to be 0.1–10 μM [14,20,21], but may increase by several fold, upon exposure to oxidants and/or deficiency of physiological antioxidants. In biological membranes, the concentration of HNE is reported to be between 10 μM and 1.0 mM following oxidative stress [22]. Local concentration of HNE in the lipid phase of oxidized low-density lipoprotein (LDL) has been estimated to be as high as 150 mM [22]. Increased concentration of free HNE and HNE-modified proteins is well documented under several pathological conditions, including autoimmune diseases [23], renal failure [14, 24], Parkinson's disease [25], alcoholic liver disease [26], and in infants with chronic lung disease [27] and atherosclerosis [28]. These adducts are often used as markers of oxidative stress.

Our studies show that erythrocytes efficiently metabolize HNE and the metabolites formed are extruded from the cells. Less than 1% HNE remains covalently bound to the cell constituents. Thus, previous immunological measurements of aldehyde-protein conjugate or even the free aldehydes are likely to be gross under estimates of the true extent of total aldehyde formation, since only a small fraction of the aldehyde escapes cellular metabolism and transport. Should there be a similar metabolic efficiency *in vivo*, the extent of aldehyde generation may be 1 to 2 orders of magnitude higher than estimated by immunoreactivity or free aldehyde measurements.

Our studies show that a major portion of HNE metabolism in erythrocytes is linked to glutathione. Approx-

imately 70% of the total HNE was metabolized through glutathione conjugation. We and others have previously shown that HNE and other structurally related lipid peroxidation-derived α -, β -unsaturated aldehydes can spontaneously form Michael adduct with GSH [3,4,29]. However, intracellular conjugation is likely to be catalyzed by glutathione-S transferase, since it enhances the rate of conjugate formation by 300–600-fold over the nonenzymatic rate [30]. Although various classes of GST could catalyze the conjugation of endogenous electrophiles, mouse GST 4-4, bovine GST 5-8, human GST 5-8, and rat GST 8-8 have high affinity for lipid peroxidation-derived α -, β -unsaturated aldehydes, particularly HNE [36,32]. However, most of the glutathionyl HNE was further metabolized in erythrocytes. The ESI⁺/MS analysis showed that the glutathione conjugate of HNE was predominantly in the reduced form as GS-DHN. Since free DHN is not electrophilic and incubation of erythrocytes with DHN did not result in the formation of GS-DHN (data not shown), it appears likely that GS-DHN originates from the enzymatic reduction of GS-HNE, rather than spontaneous addition of GSH to DHN.

Our *in vitro* studies show that the lipid peroxidation-derived aldehydes and their glutathione conjugates are efficiently reduced by the aldose reductase, and its murine analog, the fibroblast growth factor-regulated protein-1 (FR-1) [4,33]. Our molecular modeling studies suggest that the active site of aldose reductase can accommodate HNE and structurally related lipid peroxidation-derived aldehydes as well as their glutathione conjugates [4,34]. Reduced form of glutathionyl conjugates of HNE and its mercapturic acid derivatives have been detected in the rat and human urine [35,36]. A prominent role of aldose reductase in reducing the glutathione conjugates of HNE in erythrocytes is indicated by the observation that the formation of GS-DHN was significantly inhibited by two, structurally unrelated, aldose reductase inhibitors, sorbinil and tolrestat, while the alcohol dehydrogenase inhibitor 4-MP, was ineffective.

Although conjugation with glutathione attenuates the reactivity of several electrophiles, it has been reported that the glutathione conjugates of 4-hydroxy-trans-2-hexenal and nonadienal induce DNA damage [37], and that the glutathione conjugate of acrolein is more nephrotoxic than the parent aldehyde [38]. These effects have been ascribed partly to the propensity of the glutathione-aldehyde conjugates to generate free radicals [39]; an effect also observed in cells, which show increased generation of reactive oxygen species (ROS) upon exposure to HNE [40]. Thus, aldose reductase may prevent feed-forward amplification of ROS generated by lipid peroxidation products. The aldose reductase-mediated catalysis may be additionally protective, since, by reducing the aldehyde, the enzyme may prevent the spontaneous dis-

sociation of GS-HNE, which could deliver the aldehyde to nonexposed sites causing transcellular and transorgan toxicity.

Although *in vitro* aldose reductase is an efficient catalyst for the reduction of free HNE [4], the present studies show that reduction to DHN is not the major metabolic fate of HNE in erythrocytes. It is likely that the high reactivity of HNE with GSH precludes efficient reduction of free HNE by aldose reductase, and that in these and other glutathione proficient cells, aldose reductase encounters mostly the glutathione conjugate and not the free aldehyde. This is in contrast to other cells, such as hepatocytes, in which DHN formation represents 20 to 30% of the total HNE metabolism [3,41]. While hepatocytes do not express high levels of aldose reductase [42], reduction of HNE in these cells has been suggested to be catalyzed by alcohol dehydrogenase [41], which presumably due to its high catalytic rate competes with GST more efficiently than aldose reductase.

In addition to the glutathionyl conjugation, HNE in erythrocytes is also metabolized to its corresponding carboxylic acid-HNA. The HNA accounted for approximately 25% of the total metabolites. Earlier, we and others have reported that in the perfused rat heart [29], and hepatocytes [41], oxidation of HNE is catalyzed by aldehyde dehydrogenase. Mitochondrial aldehyde dehydrogenase II, in particular, has high affinity for HNE oxidation. However, because mature erythrocytes do not have mitochondria, the oxidative metabolism of HNE is unlikely to be catalyzed by aldehyde dehydrogenase in these cells. Indeed, aldehyde dehydrogenase inhibitor, cyanamide, did not provide protection against the HNE oxidation in erythrocytes. Further investigations are required to identify the metabolic pathways for the oxidation of lipid peroxidation-derived aldehydes in erythrocytes.

Acknowledgements — The technical assistance of Salisha Sobrattee in ESI⁺/MS analysis is gratefully acknowledged. This study was supported in part by National Institute of Health grants DK36118 (SKS), HL55477, and HL59378 (AB).

REFERENCES

- [1] Oranje, W. A.; Wolfenbittel, B. H. Lipid peroxidation and atherosclerosis in type II diabetes. *J. Lab. Clin. Med.* **134**:19–32; 1999.
- [2] Witz, G. Biological interactions of α -, β -unsaturated aldehydes. *Free Radic. Biol. Med.* **7**:333–349; 1989.
- [3] Esterbauer, H.; Schaur, R. J.; Zollner, H. Chemistry and biochemistry of 4-hydroxynonenal, malonaldehyde and related aldehydes. *Free Radic. Biol. Med.* **11**:81–128; 1991.
- [4] Srivastava, S.; Watowich, S. J.; Petrash, J. M.; Srivastava, S. K.; Bhatnagar, A. Structural and kinetic determinants of aldehyde reduction by aldose reductase. *Biochemistry* **38**:42–54; 1999.
- [5] Szweda, L. I.; Uchida, K.; Tsai, L.; Stadtman, E. R. Inactivation of glucose-6-phosphate dehydrogenase by 4-hydroxy-2-nonenal. Selective modification of an active-site lysine. *J. Biol. Chem.* **268**:3342–3347; 1993.
- [6] Chiu, D.; Kuypers, F.; Lubin, B. Lipid peroxidation in human red cells. *Semin. Hematol.* **26**:257–76; 1989.
- [7] Pryor, W. A. Free radicals in biological systems. In: Pryor, W. A., ed. *Free radicals in biology* (Vol. IV). New York: Academic Press; 1976:1–47.
- [8] Tappe, A. L. Oxidative fat rancidity in food products: linoleate oxidation catalyzed by hemin, hemoglobin, and cytochrome c. *Food Res.* **18**:560–572; 1953.
- [9] Hatherill, J. R.; Till, G. O.; Ward, P. A. Mechanisms of oxidant-induced changes in erythrocytes. *Agents Actions* **32**:351–358; 1991.
- [10] Chiu, D.; Lubin, B.; Shohet, S. B. Peroxidative reactions in red cell biology. In: Pryor, W. A., ed. *Free radicals in biology* (Vol. V). San Diego: Academic Press; 1982:115–160.
- [11] Drexler, H.; Hornig, B. Endothelial dysfunction in human disease. *J. Mol. Cell. Cardiol.* **31**:51–60; 1999.
- [12] Iuliano, L.; Colavita, A. R.; Leo, R.; Pratico, D.; Violi, F. Oxygen free radicals and platelet activation. *Free Radic. Biol. Med.* **22**:999–1006; 1997.
- [13] Poli, G.; Biasi, F.; Chiarotto, E.; Dianzani, M. U.; De Luca, A.; Esterbauer, H. Lipid peroxidation in human diseases: evidence of red cell oxidative stress after circulatory shock. *Free Radic. Biol. Med.* **6**:167–170; 1989.
- [14] Biasioli, S.; Schiavon, R.; De Fanti, E.; Cavalcanti, G.; Giavarina, D. The role of erythrocytes in the deperoxidative processes in people on hemodialysis. *ASAIO J.* **42**:M890–894; 1996.
- [15] Umegaki, K.; Sano, M.; Suzuki, K.; Tomita, I.; Esashi, T. Increases in 4-hydroxynonenal and hexanal in bone marrow of rats subjected to total body X-ray irradiation: association with antioxidant vitamins. *Bone Marrow Transpl.* **23**:173–178; 1999.
- [16] Ando, K.; Beppu, M.; Kikugawa, K. Evidence for accumulation of lipid hydroperoxides during the aging of human red blood cells in the circulation. *Biol. Pharm. Bull.* **18**:659–663; 1995.
- [17] Uchida, K.; Hasui, Y.; Osawa, T. Covalent attachment of 4-hydroxy-2-nonenal to erythrocyte proteins. *J. Biochem.* **122**:1246–1251; 1997.
- [18] Benedetti, A.; Comporti, M.; Esterbauer, H. Identification of 4-hydroxynonenal as a cytotoxic product originating from the peroxidation of liver microsomal lipids. *Biochim. Biophys. Acta* **620**:281–296; 1980.
- [19] Chandra, A.; Srivastava, S. K. A synthesis of 4-hydroxy-2-trans-nonenal and 4-(3H) 4-hydroxy-2-trans-nonenal. *Lipids* **32**:779–782; 1997.
- [20] Selley, M. L. Determination of the lipid peroxidation product (E)-4-hydroxy-2-nonenal in clinical samples by gas chromatography–negative-ion chemical ionization mass spectrometry of the O-pentafluorobenzyl oxime. *J. Chromatogr. B (Biomed. Sci. Appl.)* **691**:263–268; 1997.
- [21] Selley, M. L.; Bourne, D. J.; Bartlett, M. R.; Tymms, K. E.; Brook, A. S.; Duffield, A. M.; Ardlie, N. G. Occurrence of (E)-4-hydroxy-2-nonenal in plasma and synovial fluid of patients with rheumatoid arthritis and osteoarthritis. *Ann. Rheum. Dis.* **51**:481–484; 1992.
- [22] Esterbauer, H.; Ramos, P. Chemistry and pathophysiology of oxidation of LDL. *Rev. Physiol. Biochem. Pharmacol.* **127**:31–54; 1996.
- [23] Grune, T.; Michel, P.; Sitte, N.; Eggert, W.; Albrecht-Nebe, H.; Esterbauer, H.; Siems, W. G. Increased levels of 4-hydroxynonenal modified proteins in plasma of children with autoimmune diseases. *Free Radic. Biol. Med.* **23**:357–360; 1997.
- [24] Sommerburg, O.; Grune, T.; Hampl, H.; Riedel, E.; van Kuijk, F. J.; Ehrich, J. H.; Siems, W. G. Does long-term treatment of renal anemia with recombinant erythropoietin influence oxidative stress in hemodialysed patients? *Nephrol. Dial. Transpl.* **13**:2583–2587; 1998.
- [25] Selley, M. L. (E)-4-hydroxy-2-nonenal may be involved in the pathogenesis of Parkinson's disease. *Free Radic. Biol. Med.* **25**:169–174; 1998.
- [26] Aleynik, S. I.; Leo, M. A.; Aleynik, M. K.; Lieber, C. S. Increased circulating products of lipid peroxidation in patients with alco-

- holic liver disease. *Alcoholism: Clin. Exp. Res.* **22**:192–196; 1998.
- [27] Ogihara, T.; Hirano, K.; Morinobu, T.; Kim, H. S.; Hiroi, M.; Ogihara, H.; Tamai, H. Raised concentrations of aldehyde lipid peroxidation products in premature infants with chronic lung disease. *Arch. Dis. Child. (Fetal Neonatal Ed.)* **80**:F21–25; 1999.
- [28] Uchida, K.; Toyokuni, S.; Nishikawa, K.; Kawakishi, S.; Oda, H.; Hiai, H.; Stadtman, E. R. Michael addition-type 4-hydroxy-2-nonenal adducts in modified low-density lipoproteins: markers for atherosclerosis. *Biochemistry* **33**:12487–12494; 1994.
- [29] Srivastava, S.; Chandra, A.; Wang, L. F.; Seifert, W. E. Jr.; DaGue, B. B.; Ansari, N. H.; Srivastava, S. K.; Bhatnagar, A. Metabolism of the lipid peroxidation product, 4-hydroxy-trans-2-nonenal, in isolated perfused rat heart. *J. Biol. Chem.* **273**:10893–10900; 1998.
- [30] Alin, P.; Danielson, U. H.; Mannervik, B. 4-Hydroxyalk-2-enals are substrates for glutathione transferase. *FEBS Lett.* **179**:267–270; 1985.
- [31] Zimniak, P.; Singhal, S. S.; Srivastava, S. K.; Awasthi, S.; Sharma, R.; Hayden, J. B.; Awasthi, Y. C. Estimation of genomic complexity, heterologous expression, and enzymatic characterization of mouse glutathione S-transferase mGSTA4-4 (GST 5.7). *J. Biol. Chem.* **269**:992–1000; 1994.
- [32] He, N.; Singhal, S. S.; Awasthi, S.; Zhao, T.; Boor, P. J. Role of glutathione S-transferase 8-8 in allylamine resistance of vascular smooth muscle cells in vitro. *Toxicol. Appl. Pharm.* **158**:177–185; 1999 .
- [33] Srivastava, S.; Harter, T. M.; Chandra, A.; Bhatnagar, A.; Srivastava, S. K.; Petrash, J. M. Kinetic studies of FR-1, a growth factor-inducible aldo-keto reductase. *Biochemistry* **37**:12909–12917; 1998.
- [34] Dixit, B. L.; Balendriran, G. K; Watowich, S. J.; Srivastava, S.; Ramana, K. V.; Petrash, J. M.; Bhatnagar, A.; Srivastava, S. K. Kinetic and structural characterization of the glutathione binding site of aldose reductase. *J. Biol. Chem.* **275**:21587–21595; 2000.
- [35] Alary, J.; Debrauwer, L.; Fernandez, Y.; Cravedi, J. P.; Rao, D.; Bories, G. 1,4-Dihydroxynonene mercapturic acid, the major end metabolite of exogenous 4-hydroxy-2-nonenal, is a physiological component of rat and human urine. *Chem. Res. Toxicol.* **11**:130–135; 1998.
- [36] Laurent, A.; Alary, J.; Debrauwer, L.; Cravedi, J. P. Analysis in the rat of 4-hydroxynonenal metabolites excreted in bile: evidence of enterohepatic circulation of these byproducts of lipid peroxidation. *Chem. Res. Toxicol.* **12**:887–894; 1999.
- [37] Eisenbrand, G.; Schuhmacher, J.; Golzer, P. The influence of glutathione and detoxifying enzymes on DNA damage induced by 2-alkenals in primary rat hepatocytes and human lymphoblastoid cells. *Chem. Res. Toxicol.* **8**:40–46; 1995.
- [38] Horvath, J. J.; Witmer, C. M.; Witz, G. Nephrotoxicity of the 1:1 acrolein-glutathione adduct in the rat. *Toxicol. Appl. Pharm.* **117**:200–207; 1992.
- [39] Adams, J. D. Jr.; Klaidman, L. K. Acrolein-induced oxygen radical formation. *Free Radic. Biol. Med.* **15**:187–193; 1993.
- [40] Uchida, K.; Shiraishi, M.; Naito, Y.; Torii, Y.; Nakamura, Y.; Osawa, T. Activation of stress signaling pathways by the end product of lipid peroxidation. 4-hydroxy-2-nonenal is a potential inducer of intracellular peroxide production. *J. Biol. Chem.* **274**:2234–2242; 1999.
- [41] Hartley, D. P.; Ruth, J. A.; Petersen, D. R. The hepatocellular metabolism of 4-hydroxynonenal by alcohol dehydrogenase, aldehyde dehydrogenase, and glutathione S-transferase. *Arch. Biochem. Biophys.* **316**:197–205; 1995.
- [42] Iwata, T.; Sato, S.; Jimenez, J.; McGowan, M.; Moroni, M.; Dey, A.; Ibaraki, N.; Reddy, V. N.; Carper, D. Osmotic response element is required for the induction of aldose reductase by tumor necrosis factor α . *J. Biol. Chem.* **274**:7993–8001; 1999.